

Transient rheology of a polyethylene melt under shear

J. D. Moore,^{1,2} S. T. Cui,^{1,2} H. D. Cochran,^{1,2} and P. T. Cummings^{1,2,3}

¹Department of Chemical Engineering, University of Tennessee, Knoxville, Tennessee 37996-2200

²Chemical Technology Division, Oak Ridge National Laboratory, Oak Ridge, Tennessee 37831-6268

³Department of Chemistry and Department of Computer Science, University of Tennessee, Knoxville, Tennessee 37996-2200

(Received 4 June, 1999)

Using nonequilibrium molecular dynamics simulation, we have studied the response of a C_{100} model polymer melt to a step change from equilibrium to a constant, high shear rate flow. The transient shear stress of the model polymer melt exhibits pronounced overshoot at the strain value predicted by the reptation model, in striking similarity to melts of longer, entangled polymer governed by reptation motion. At the maximum of shear stress overshoot, the molecular orientational order and the alignment angle are found to be midway between those characteristic of Newtonian flow and full alignment with the flow. The Doi-Edwards theory is found to be applicable but only by taking into account the shear-rate-dependence of the terminal relaxation time. We further analyze the molecular origins of such behavior in short polymer chains by decomposing the total stress into the contributions from various molecular interactions. [S1063-651X(99)08911-4]

PACS number(s): 83.20.Jp, 83.20.Di, 83.20.Fk, 83.50.By

The rheological properties of a liquid of short, unentangled polymer chains at high shear rate are still not well understood. Experimental data are unavailable because of the difficulty of reaching the nonlinear viscoelastic regime in shear rate for short-chain systems. On the theoretical side, a successful theory of the rheological properties of short-chain polymers in the nonlinear regime has not been developed. The Rouse model is generally considered to provide a good description of the linear-response dynamics of short-chain polymeric systems in the liquid state [1]. This is substantiated by a large body of experimental work and molecular simulation results. Recent computer simulation studies suggest that the linear alkanes, in chain lengths of up to 100 carbon atoms, are well described by the Rouse model, which accurately predicts the self-diffusion, segmental orientations, and equilibrium viscosity [2–4]. However, the Rouse model is essentially a linear theory with regard to the prediction of rheological properties. Its prediction of the nonlinear rheological response is qualitatively incorrect. For example, within the Rouse model, the viscosity is Newtonian at all shear rates $\dot{\gamma}$, contrary to the simulation results, where shear-thinning has been observed at high shear rate. For the response to a step change from equilibrium to a constant, high shear rate (i.e., $\dot{\gamma}=0$ for $t<0$, $\dot{\gamma}=$ a fixed positive value for $t\geq 0$), the Rouse model predicts a linear response in both shear stress and first normal stress that is independent of the magnitude of shear deformation [1].

Reptation theory is generally considered to apply only to systems of high molecular weight polymers where entanglements exist [1,5]. The well-known predictions of the theory for entangled polymeric liquids include viscoelastic behavior and the strong power law dependence of the Newtonian viscosity on the molecular weight $\eta\propto M^3$. The reptation model also predicts a well defined transient response when a polymeric liquid is subjected to shear deformation. The original Doi-Edwards (DE) model predicts that for sufficiently high step shear start up ($\dot{\gamma}\tau_d>2$, where τ_d is the disentanglement or reptation time), the shear stress exhibits an overshoot at a total strain $\gamma\equiv\int\dot{\gamma}dt=\dot{\gamma}t$ of about 2.0 and no overshoot in

the normal stress difference [6]. An improved theory by Pearson *et al.* predicts a shear stress overshoot at a total strain of 2.3 and normal stress overshoot at 4.3 [7]. These predictions have been corroborated by experiments [8]. Pearson *et al.* [7] provide a concise summary of the behavior of entangled polymers during the start-up of steady shearing. Recently, effort has been made by a number of authors [9–16] to modify DE in order to improve its predictions for various aspects of the nonlinear viscoelasticity of entangled polymer melts in general and to achieve consistency with the empirical Cox-Merz rule in particular [9–12].

Our interest is in gaining a molecular-level understanding of the non-Newtonian rheology of alkane liquids and polymers using molecular models that preserve as much as possible of the details of the intermolecular interactions and intramolecular architecture [17,18]. Molecular simulation studies of the rheology of polymeric systems have usually been limited to very small system sizes, short time-scales, simplified polymer models, and/or coarse-grained simulation techniques. Recently, equilibrium molecular dynamics (EMD) simulations of reasonably long-chain alkane liquids have been reported (e.g., $C_{100}H_{202}$) [2,3] using the same types of realistic united atom [3,19,20] and explicit atom [21] potential models that have been used extensively to study shorter liquid alkanes. The feasibility of EMD calculations on $C_{100}H_{202}$ led us to perform nonequilibrium molecular dynamics (NEMD) simulations of a $C_{100}H_{202}$ melt.

We report NEMD [22,23] simulations of a monodisperse $C_{100}H_{202}$ melt utilizing the united atom potential model developed by Siepmann *et al.* [20] and reversible reference system propagator algorithm (RRESPA) multipletime-step dynamics [24–26]. This represents the longest alkane chain to which NEMD has been applied using a realistic united atom model, and in this paper we focus on the transient rheological response to constant shear-rate start-up tests. The slld equations of motion [22] (incorporating a Nosé thermostat) were used to simulate $C_{100}H_{202}$ under planar Couette flow. They were integrated using a multiple-time-step technique [24,26]. All of the intramolecular interactions were treated as fast motions (smaller time step of 0.47 fs) and the intermo-

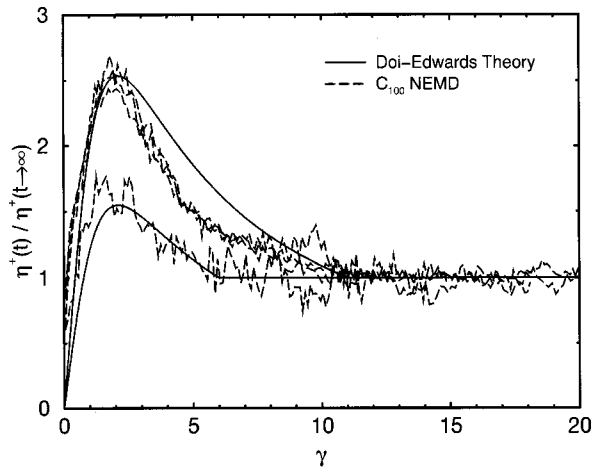


FIG. 1. Shear stress growth coefficient normalized by its steady-state value as a function of total strain. Solid lines are the Doi-Edwards theory with $\dot{\gamma}\tau_d=6$ (lower curve) and $\dot{\gamma}\tau_d=11$ (upper curve). Dashed lines are the C_{100} simulation data for 4 strain rates between 4.3×10^{11} and $4.3 \times 10^9 \text{ s}^{-1}$ inclusive.

lecular interaction as the slow motion (larger time step of 2.35 fs). Since the streaming velocity is applied to the atomic sites in our NEMD simulation, we calculate the pressure tensor \mathbf{P} according to the atomic formalism. The simulations involved 400 $C_{100}H_{202}$ molecules (i.e., 40 000 united atoms) at a temperature of 448 K and $\rho=0.75 \text{ g/mL}$, estimated from the experimental data in Pearson *et al.* [27]. The simulation box measured 85.3 Å in the y - and z -directions but 170.6 Å in the x -direction (i.e., the shear direction). The system was equilibrated for 12.6 ns (approximately 4 rotational relaxation times (τ_R) as estimated from our EMD simulations). Subsequent to equilibration, we used NEMD to perform constant shear-rate start-up tests on our C_{100} melt. The approach of the various growth coefficients (viscosity $\eta^+(t, \dot{\gamma})$, first normal stress difference $\Psi_1^+(t, \dot{\gamma})$, and second normal stress difference $\Psi_2^+(t, \dot{\gamma})$, where the + superscript indicates the value of the quantity after start-up of shear at time $t=0$) to their steady-state values was studied.

Direct comparison between simulation and DE theory [1,6] is made in Fig. 1. As in DE theory, the shear stress growth coefficients in the simulations pass through maxima before reaching steady-state. The maximum in the overshoot occurs at a constant value of $\dot{\gamma}t \approx 2$. At the three highest strain rates, the maximum in normalized stress overshoot is ≈ 2.6 , and at the smallest shear rate it is ≈ 1.7 . The theory predicts the location of the peak in the overshoot at $\dot{\gamma}t \approx 2$, in quantitative agreement with simulation. In DE theory, the steady-state viscosity is reached in the amount of time τ_d , so it was necessary to choose two different values of the product $\dot{\gamma}\tau_d$ (as given in the caption of Fig. 1) in order to reconcile the theoretical predictions with the simulation results. This implies that $\tau_d \approx 1.4 \times 10^{-9} \text{ s}$, $2.9 \times 10^{-10} \text{ s}$, $7.2 \times 10^{-11} \text{ s}$, $2.6 \times 10^{-11} \text{ s}$ at strain rates $\dot{\gamma} = 4.3 \times 10^9 \text{ s}^{-1}$, $3.8 \times 10^{10} \text{ s}^{-1}$, $1.5 \times 10^{11} \text{ s}^{-1}$, $4.3 \times 10^{11} \text{ s}^{-1}$, respectively, and that at the three highest strain rates $\tau_d \propto 1/\dot{\gamma}$. These values of τ_d are much less than the value usually used in DE theory [1,6]. In the theory, τ_d is estimated on the basis of the time taken for a polymer molecule to move through a

distance equal to its own length in a tube created by the surrounding polymer molecules, calculated in the absence of shear based on diffusive motion through the tube. The small effective values of τ_d needed to fit the high-shear-rate simulation results are consistent with the idea that at high shear rate the time taken for a molecule to move through its own length is much less. This would be true whether the tube is considered to be fixed in space so that the relevant motion is assumed to be convective in the flow field (in which case $\tau_d \propto 1/\dot{\gamma}$) or the tube is considered to convect in the flow field in which case the relevant motion is diffusive within the tube (and the diffusion coefficient can be expected to increase on the basis of results for simple fluids in nonlinear shear [28]). Whether the change in diffusion coefficient with strain rate is large enough to explain the large changes in τ_d is currently under investigation in our group. Very preliminary results [29] suggest that indeed the strain-rate-dependent diffusion coefficient may very well increase proportional to $\dot{\gamma}$ at high $\dot{\gamma}$. In contrast to this possible diffusive explanation, Marrucci has proposed that the mechanism of ‘‘convective constraint release’’ (CCR) could result in a relaxation time that decreases linearly with increasing $\dot{\gamma}$ under fast flow conditions for entangled systems [9], though Mhetar and Archer argue that CCR might lead to a renewal time that is either unchanged or increases with increasing $\dot{\gamma}$ [12]. Although not shown in the figure, we also performed a comparison between our simulation results and experiment on high-density polyethylene (HDPE) reported in Refs. [30,31]. The HDPE sample consisted of linear molecules with $\bar{M}_w = 104\,000 \text{ g/mol}$ and $\bar{M}_n = 18\,900 \text{ g/mol}$ [30], two orders of magnitude and one order of magnitude larger than our system, respectively. The overshoot seen in the simulations is stronger than that seen in the experiments. Nevertheless, qualitative agreement is seen in that the peak in the stress growth coefficient occurs at similar values of the total strain and the strength of the stress overshoot tends to increase with increasing strain rate.

We would like to gain molecular-level insight into the stress overshoot phenomena which have been linked in the literature to the stretching of the chains in the flow field. Since our simulations show that the value of $\dot{\gamma}t$ corresponding to the maximum in the chain dimension R_g is much delayed ($\dot{\gamma}t \approx 8-15$) compared to the maximum in the shear stress and varies with strain rate when the location of the maximum shear stress does not, we would like to determine if the location of the shear stress maximum can be correlated more intimately with some other related property.

For shorter alkane chains, if the strain rate exceeds the critical value ($\dot{\gamma}_c \approx 1/\tau_R$, where τ_R is the rotational relaxation time), shear thinning occurs and is accompanied by the alignment of molecules with the flow direction as measured by the liquid crystal order tensor [18,32,33]. The eigenvector corresponding to the largest eigenvalue (the order parameter) of the order tensor gives the preferential orientation of the molecules relative to the flow field. In Fig. 2 the alignment angle is plotted vs. total strain γ for the C_{100} system at the four different strain rates under constant shear-rate start-up tests. The alignment angle decreases with increasing strain and approaches a small limiting value at long times, evi-

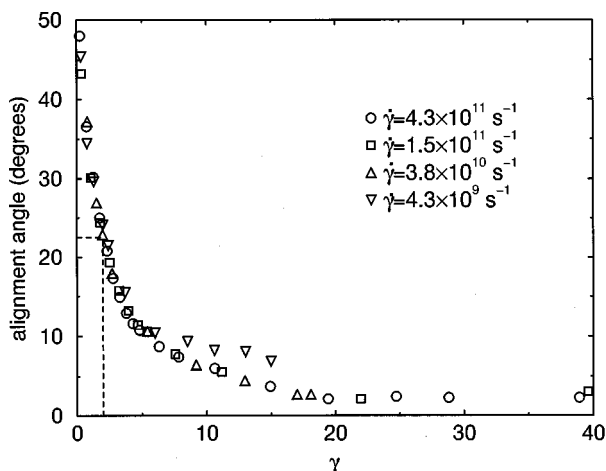


FIG. 2. The alignment angle with the flow field of the C_{100} end-to-end vector vs total strain for four different strain rates under constant shear-rate start-up tests. The purpose of the dashed lines is to emphasize the fact that alignment angle has reached half its linear-regime value at $\dot{\gamma}t \approx 2$.

dence of extreme alignment in the flow field. The dashed lines in Fig. 2 illustrate that at all four strain rates the alignment angle is approximately one-half its linear-regime value of 45° at $\gamma \approx 2$. That is, the C_{100} melt experiences its maximum shear stress when it has been strained enough to be at the midpoint of the shear-alignment process. Also, at $\dot{\gamma}t \approx 2$, the order parameter in the C_{100} system is equal to 0.5, half way between the limiting values of 1 (complete order) and 0 (complete disorder).

Finally, it is informative to decompose the shear stress overshoot curve into the components arising from the various contributions to the shear stress. In Fig. 3 these contributions are plotted versus total strain under constant shear-rate start-up test at $\dot{\gamma} = 4.3 \times 10^{11} \text{ s}^{-1}$, averaged over 3 independent constant shear-rate start-up simulations. All six contributions pass through extrema during their approach to steady state. The kinetic and torsional contributions pass through minima. The Lennard-Jones (LJ), both intramolecular and intermolecular, and bond-stretching contributions all

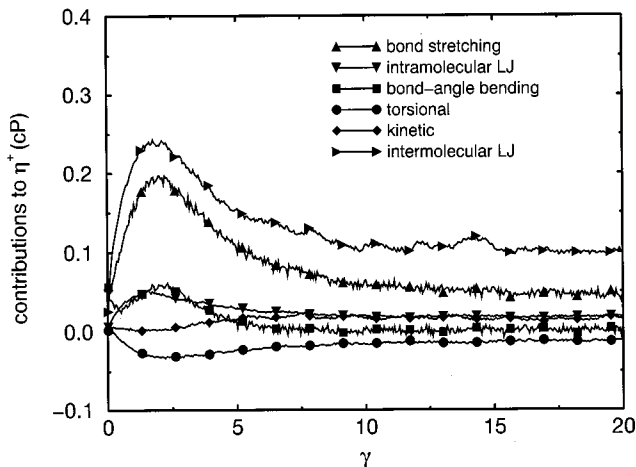


FIG. 3. Contributions to the shear stress growth coefficient of the C_{100} melt under constant shear-rate start-up test at $\dot{\gamma} = 4.3 \times 10^{11} \text{ s}^{-1}$.

pass through maxima at $\dot{\gamma}t \approx 2$. The bond-angle-bending contribution passes through a minimum followed by a maximum. Clearly, the bond-stretching and intermolecular-LJ contributions dominate the stress overshoot. The former provides confirmation that the stress overshoot is closely related to the stretching of the individual chain-segments under the influence of the flow field. The latter suggests that, as the chains are being straightened-out and aligned, the shearing of molecules past one another causes strong intermolecular “frictional” interactions that also contribute significantly to the transient behavior of the shear stress.

In summary, NEMD simulation techniques have been applied to study a C_{100} melt which exhibits pronounced transients in its response to constant shear-rate start-up that agree qualitatively with experimental observations. Though the C_{100} system is too short to experience the sort of entanglements on which DE theory is based, the results are in good quantitative agreement with DE theory if τ_d is assumed to be strain-rate dependent. The NEMD simulations demonstrate that the stress overshoot in this C_{100} melt is intimately related to the molecular alignment induced by the shear field and is dominated by bond-stretching and intermolecular-LJ contributions.

It is worth considering the question of why the reptation model should be applicable to a melt of C_{100} alkane molecules. The physical picture underlying the reptation model of de Gennes (and the DE theory and its derivatives which are based on it) is that very long chain molecules become so entangled that the only mechanism of (center of mass) chain motion is by “reptation” motion in which one end of the chain moves into a near-by region of free volume, and the rest of the chain is constrained to follow snake-like through the tubular volume occupied by the chain itself because all of the surrounding volume is occupied by slowly moving segments. Usually, it is thought that the reptation model does not apply to the motion of shorter chain molecules ($C_n, n \lesssim 300$ [34]) because they are too short to become entangled. In our high strain rate simulations (but at strain rates encountered in severe lubrication applications) the rate of center of mass chain motion (due to shear) is fast compared to the rate of motion due to diffusion. Thus, at these high strain rates, the reptation picture may be accurate even for relatively short chains without entanglements because of the order induced by the strain field such that the chains follow their own contour. However, as we have seen, it is only applicable when the terminal relaxation time is modified to take into account the high shear rates.

The authors would like to thank Professor M. H. Wagner for providing access to the HDPE experimental data and Professor R. B. Bird and Professor M. D. Dadmun for helpful discussions. This research is made possible by a substantial grant of Cray T3E computer time by the National Energy Research Scientific Computing Center. Additional calculations were performed on Cray T3E supercomputers located at Cray Research in Eagan, MN, and on the Intel Paragons at the Center for Computational Sciences at Oak Ridge National Laboratory. This work was supported in part by the Division of Materials Sciences of the U. S. Department of Energy. Oak Ridge National Laboratory is operated for the Department of Energy by Lockheed Martin Energy Research Corp. under Contract No. DE-AC05-96OR22464.

- [1] M. Doi and S. Edwards, *The Theory of Polymer Dynamics* (Oxford, New York, 1988).
- [2] W. Paul, G.D. Smith, D.Y. Yoon, B. Farago, S. Rathgeber, A. Zirkel, L. Willner, and D. Richter, *Phys. Rev. Lett.* **80**, 2346 (1998).
- [3] V.A. Harmandaris, V.G. Mavrantzas, and D.N. Theodorou, *Macromolecules* **31**, 7934 (1998).
- [4] M. Mondello, G.S. Grest, E.B. Webb III, P. Peczak, *J. Chem. Phys.* **109**, 798 (1998).
- [5] P.G. de Gennes, *J. Chem. Phys.* **55**, 572 (1971).
- [6] M. Doi and S. Edwards, *J. Chem. Soc., Faraday Trans. 2* **74** 1789 (1978); **74** 1802 (1978); **74** 1818 (1978); **75** 38 (1979).
- [7] D. Pearson, E. Herbolzheimer, N. Grizzuti, and G. Marrucci, *J. Polym. Sci., Part B: Polym. Phys.* **29**, 1589 (1991).
- [8] E.V. Menezes and W.W. Graessley, *J. Polym. Sci., Polym. Phys. Ed.* **20**, 1817 (1982).
- [9] G. Marrucci, *J. Non-Newtonian Fluid Mech.* **62**, 279 (1996).
- [10] G. Ianniruberto and G. Marrucci, *J. Non-Newtonian Fluid Mech.* **65**, 241 (1996).
- [11] G. Marrucci and G. Ianniruberto, *J. Non-Newtonian Fluid Mech.* **82**, 275 (1999).
- [12] V. Mhetar and L.A. Archer, *J. Non-Newtonian Fluid Mech.* **81**, 71 (1999).
- [13] A. Ait-Kadi, A. Ramazani, M. Grmela, and C. Zhou, *J. Rheol.* **43**, 51 (1999).
- [14] J. Remmelgas, G. Harrison, and L.G. Leal, *J. Non-Newtonian Fluid Mech.* **80**, 115, 1999.
- [15] D.W. Mead, R.G. Larson, and M. Doi, *Macromolecules* **31**, 7895 (1998).
- [16] H.C. Öttinger and A.N. Beris, *J. Chem. Phys.* **110**, 6593 (1999).
- [17] J.D. Moore, S.T. Cui, P.T. Cummings, and H.D. Cochran, *AIChE. J.* **43**, 3260 (1997).
- [18] S.T. Cui, P.T. Cummings, H.D. Cochran, J.D. Moore, and S.A. Gupta, *Int. J. Thermophys.* **19**, 449 (1998).
- [19] W. Paul, D.Y. Yoon, and G.D. Smith, *J. Chem. Phys.* **103**, 1702 (1995).
- [20] J.I. Siepman, S. Karaborni, and B. Smit, *Nature (London)* **365**, 330 (1993).
- [21] G.D. Smith and D.Y. Yoon, *J. Chem. Phys.* **100**, 649 (1994).
- [22] D.J. Evans and G.P. Morriss, *Statistical Mechanics of Non-equilibrium Liquids* (Academic, London, 1990).
- [23] S. Sarman, D.J. Evans, and P.T. Cummings, *Phys. Rep.* **305**, 1 (1998).
- [24] M.E. Tuckerman, B.J. Berne, and G.J. Martyna, *J. Chem. Phys.* **97**, 1990 (1992).
- [25] C.J. Mundy, J.I. Siepman, and M.L. Klein, *J. Chem. Phys.* **102**, 3376 (1995).
- [26] S.T. Cui, P.T. Cummings, and H.D. Cochran, *J. Chem. Phys.* **104**, 255 (1996).
- [27] D.S. Pearson, G. Ver Strate, E. von Meerwall, and F.C. Schilling, *Macromolecules* **20**, 1133 (1987).
- [28] P.T. Cummings, B.Y. Wang, D.J. Evans, and K.J. Fraser, *J. Chem. Phys.* **94**, 2149 (1991).
- [29] J.D. Moore, S.T. Cui, H.D. Cochran, and P.T. Cummings (unpublished).
- [30] M.H. Wagner, H. Bastian, P. Ehrecke, M. Kraft, P. Hachmann, and J. Meissner, *J. Non-Newtonian Fluid Mech.* **79**, 283 (1998).
- [31] M. Kraft, Dissertation ETH Zürich Nr. 11 417 (1996).
- [32] S. Chandrasekhar, *Liquid Crystals* (Cambridge University Press, Cambridge, England, 1992).
- [33] P.G. de Gennes and J. Prost, *The Physics of Liquid Crystals* (Clarendon Press, Oxford, 1993).
- [34] S. Matsuoka and T.K. Kwei, in *Macromolecules. An Introduction to Polymer Science*, edited by F.A. Bovey and F.H. Winslow, p. 347 (Academic Press, New York, 1979).